INTRABEAM SCATTERING IN THE CERN ANTIPROTON ACCUMULATOR

M. CONTE

Dipartimento di Fisica, Università di Genova, INFN, Sezione di Genova, Via Dodecaneso 33, I-16146 Genova, Italy

and

M. MARTINI

PS Division, CERN, CH-1211 Genève 23, Switzerland

The existing theories of intrabeam scattering, valid for high-energy rings ($\gamma \geqslant 10$), are improved and modified to give results applicable to the CERN Antiproton Accumulator (AA), which operates at lower energies ($\gamma \simeq 3.77$).

A comparison is made between theoretical evaluations and measured data, gathered by loading the AA with high-intensity proton beams. The agreement obtained is rather satisfactory and this represents the first experimental check of the most up to date intrabeam-scattering theories.

1. INTRODUCTION

The goal of the recently approved Antiproton Collector[1] (ACOL) at CERN is to increase the daily $\bar{p}$ yield by a factor at least ten. As a consequence, the existing Antiproton Accumulator[2] (AA) will be loaded by a number of antiprotons greater than that attained so far. The stored current and its brightness are limited by intrabeam scattering.

In order to perform reliable theoretical forecasts, the original Piwinski[3] theory has been extended[4] by taking into account the variation of betatron functions and momentum dispersion function along the lattice.

Concurrently, another approach has been followed by Bjorken and Mtingwa[5] at Fermilab. Emittance growth-rates are evaluated by means of a scattering-matrix formalism, considering the variations of dispersion and beta-functions, but making approximations valid for ultrarelativistic beams only.

In this paper, the Bjorken–Mtingwa theory is adapted to deal with lower-energy beams. The approximations made in their original work are not used here, thus obtaining final formulae with a higher degree of reliability at low energy.

Results obtained from these formulae are compared with predictions based upon the existing theories[3-5] mentioned above, then comparisons are made between these results and recent experimental data gathered during operation of the Antiproton Accumulator.
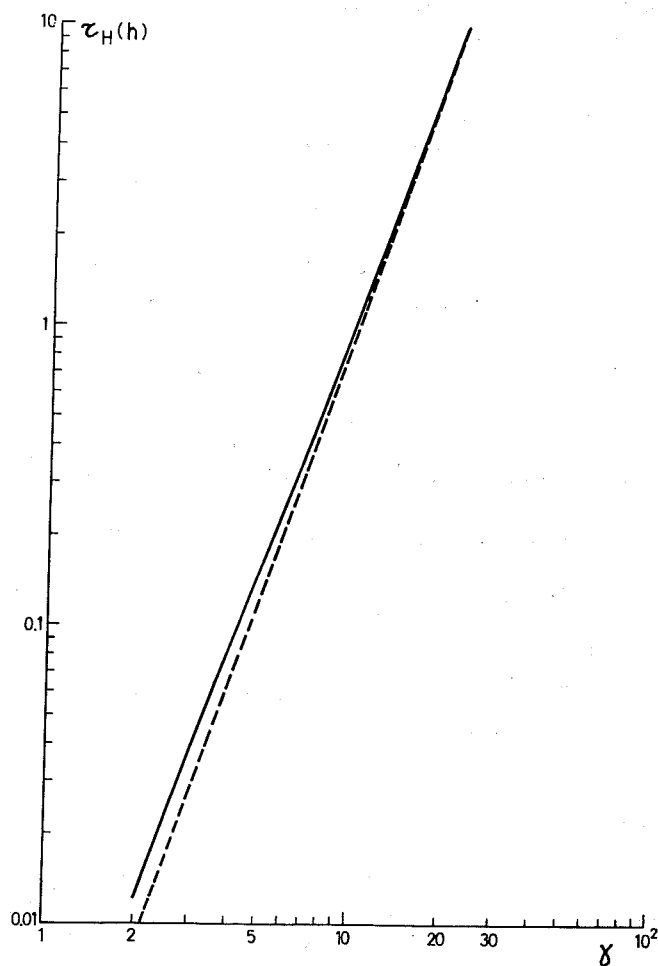
FIGURE 1   Plots of τ_H vs γ: solid (broken) line refers to the Bjorken–Mtingwa approach without (with) approximations.

2. GROWTH-RATES EVALUATION

Growth rates of the horizontal emittance ε_H and the vertical one ε_V are by definition

$$\frac{1}{\tau_H} = \frac{1}{\varepsilon_H} \frac{d\varepsilon_H}{dt} \tag{1.a}$$

$$\frac{1}{\tau_V} = \frac{1}{\varepsilon_V} \frac{d\varepsilon_V}{dt}, \tag{1.b}$$

while the growth-rate of the longitudinal phase-plane area A_{ph} is

$$\frac{1}{\tau_E} = \frac{1}{A_{\mathrm{ph}}} \frac{dA_{\mathrm{ph}}}{dt}. \tag{1.c}$$

Relativistic scattering theory provides the general formula [see Eq. (3.4) of Ref. 5]

$$\frac{1}{\tau_a} = A \left\langle \int_0^\infty (\text{Tr } L^{(a)} \text{Tr } M^{-1} - 3 \text{ Tr } (L^{(a)} M^{-1})) \frac{\lambda^{1/2} \, d\lambda}{(\det M)^{1/2}} \right\rangle, \tag{2}$$

where $a = H, V, E$ and the brackets $\langle \cdots \rangle$ denote an average around the ring.

More details are given in the Appendix, where the growth rates are shown without high-energy approximation.

A FORTRAN program has been written in order to evaluate integrals and to perform the averages that give rise to the three growth rates. For comparison, another program has been written, adopting the same approximate growth rates as in Ref. 5. Several cases have been worked out, all with the same parameters as in Ref. 6, but with varying $\bar{p}$ energy (γ). Figure 1 shows how a plot of the τ_H
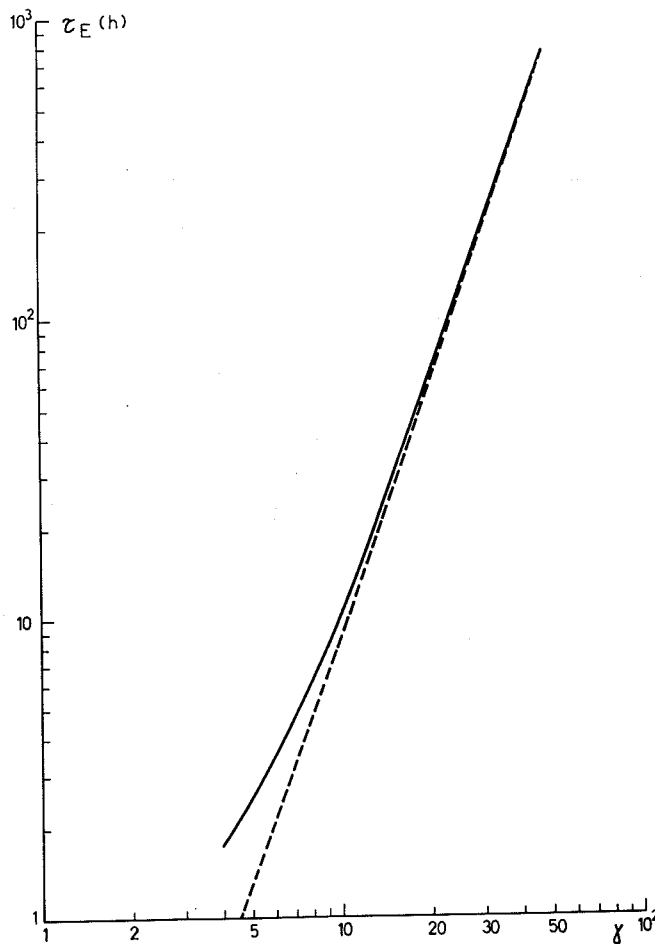

FIGURE 2   Plots of τ_E vs γ: solid (broken) line refers to the Bjorken–Mtingwa approach without (with) approximations.

values computed without approximation (solid line) tends to overlap the approximate plot (broken line) for $\gamma \geqslant 10$. The same overlap occurs for values of τ_E found by means of both approaches, as shown in Fig. 2.

Values of τ_V shown in Fig. 3 ($\gamma > 10$) are negative: this means that damping in the vertical motion compensates the growth of horizontal and longitudinal oscillations. However, the two plots exhibit the same overlapping as in the previous examples. Both programs predict a change of sign of τ_V for values of γ around 6: a plot of the growth rate $1/\tau_V$ vs γ (Fig. 4) illustrates how, for increasing γ, this growth rate decreases, becoming first steady ($|\tau_V| \simeq \infty$) and then negative, indicating that a certain amount of shrinkage or damping is taking place, as energy is transferred to other degrees of freedom.
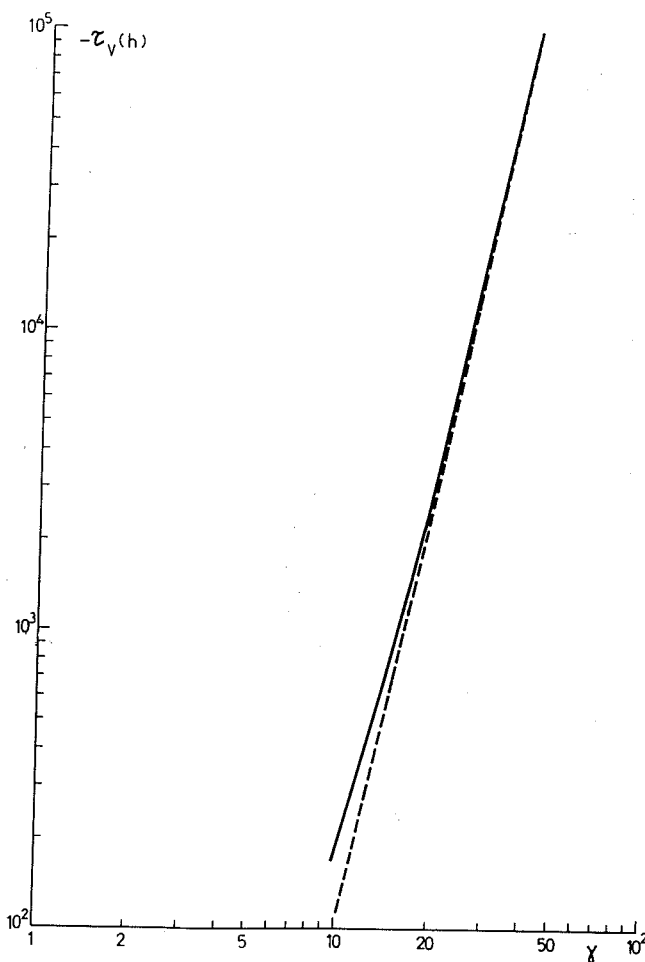

FIGURE 3   Plots of $-\tau_V$ vs γ: solid (broken) line refers to the Bjorken–Mtingwa approach without (with) approximations.
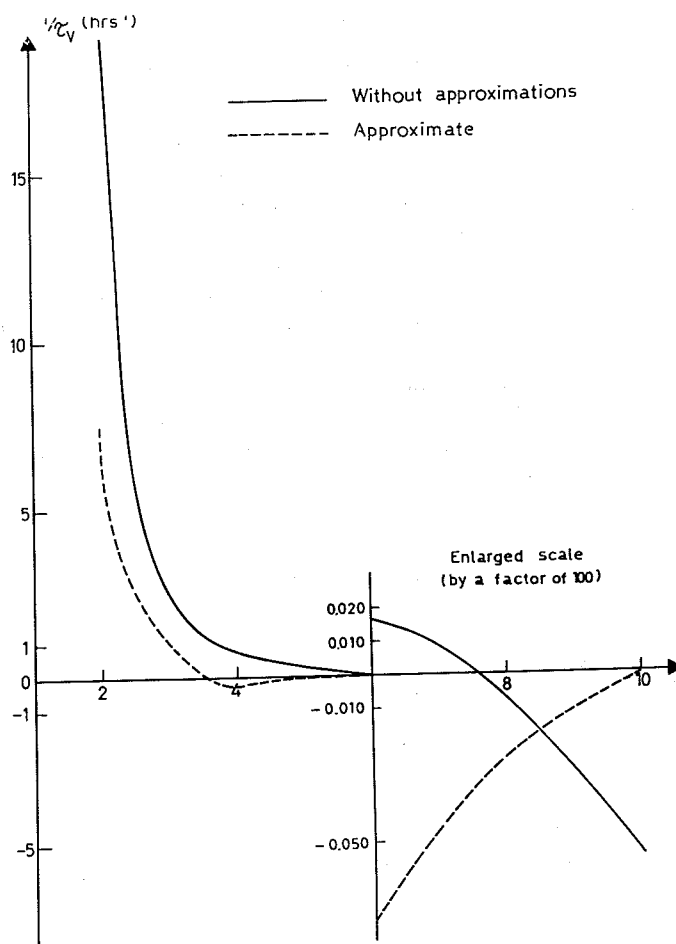
FIGURE 4   Plot of $1/\tau_V$ vs γ, with a magnification equal to 100 for $6 \leqslant \gamma \leqslant 10$.

After these comparisons, which check the level of reliability of the approximations made in Ref. 5, the program without approximation was compared with results obtained via the extended Piwinski theory.[4]

Take note that Piwinski's theory defines as growth rates the logarithmic derivatives of the rms betatron-angle values σ_H' and σ_V'; while the growth rates defined both in the Bjorken–Mtingwa work and in this paper are the logarithmic derivatives of the transverse emittances ε_H and ε_V [see Eq. (1.a, b)]. Since the emittance is proportional to σ^2 there is a factor between these formulas

$$(\tau_{H,V})_{\text{Betatron Angle}} = 2(\tau_{H,V})_{\text{Emittance}}. \tag{3}$$

On the other hand, τ_E is defined in the same way in all treatments, hence

$$(\tau_E)_{\text{Momentum Spread}} = (\tau_E)_{\text{Phase Plane}}. \tag{4}$$

TABLE I

Growth Rates from Different Theories

		Horizontal	Vertical	Longitudinal (Energy)
τ_{Piwinski}	(h)	0.150	1.62	1.70
$\tau_{\text{Bjorken–Mtingwa}}$	(h)	0.078	0.94	1.73

The agreement between the two different theoretical approaches is very satisfactory, provided that conditions (3) and (4) are taken into account.

Table I gathers the results obtained from a program based upon the extended[4] Piwinski theory and one based on the elaboration of the Bjorken–Mtingwa theory[5] made in this work. Input data are the beam characteristics and the lattice parameters pertaining to the AA in the design[2] goals:

$$N = 6 \times 10^{11} \text{ antiprotons}$$

$$\varepsilon_H = 1.4\pi \text{ mm mrad}$$

$$\varepsilon_V = 1.0\pi \text{ mm mrad}$$

$$\frac{\Delta p}{p} = \pm 1.5 \times 10^{-3}$$

$$\gamma = 3.7722,$$

plus other data given in Ref. 6.

The emittances mentioned above are measured by scarping 95% of the beam and are related to the σ's of the projected distribution by the well-known formula

$$\varepsilon_{H,V} = \frac{6\beta_{H,V}\sigma'^2_{H,V}}{1 + \alpha^2_{H,V}}$$

3. EXPERIMENTS

We describe now the experiments in which beam enlargement due to multiple Coulomb scattering has been observed. A dense proton beam was stacked in the CERN Antiproton Accumulator during a machine experiment,[7] with only the high-frequency cooling system switched on. The stack was then left cooling down until it became steady, i.e., until a balance occurred between cooling and intrabeam scattering. The stable-beam parameters achieved were

$$N = 6.01 \times 10^{11} \text{ protons } (\gamma = 3.7722 \text{ at } 3.41 \text{ GeV/c})$$

$$\varepsilon_H = 3.9\pi \text{ mm mrad}$$

$$\varepsilon_V = 7.6\pi \text{ mm mrad}$$

$$\frac{\Delta p}{p} = \pm 1.9 \times 10^{-3} \text{ (or } \Delta f_{\text{rms}} = 154 \text{ Hz)}$$

Afterwards, the cooling was switched off and the proton stack was left to blow up in the transverse and longitudinal planes. The changes of emittances and momentum dispersion were observed every 5 minutes for about 8 hours. Figure 5 is a semilog plot of the evolutions of the emittances ε_H and ε_V (at 95% of particles in the phase-space), together with the rms frequency (half) stack width Δf_{rms}. Zero time corresponds to when the cooling was switched off.

It is worthwhile to emphasize that the emittances were measured by means of a Schottky pickup and a spectrum analyzer, where the sidebands were analyzed using a calibration factor, which was fixed by performing an emittance measurement with scrapers.

Note also that $\Delta f_{rms} = 1.58 \times 10^5 (\Delta p/p)_{rms}$, where the coefficient of proportionality is the product of the stack center frequency times the η-function, from Ref. 6.
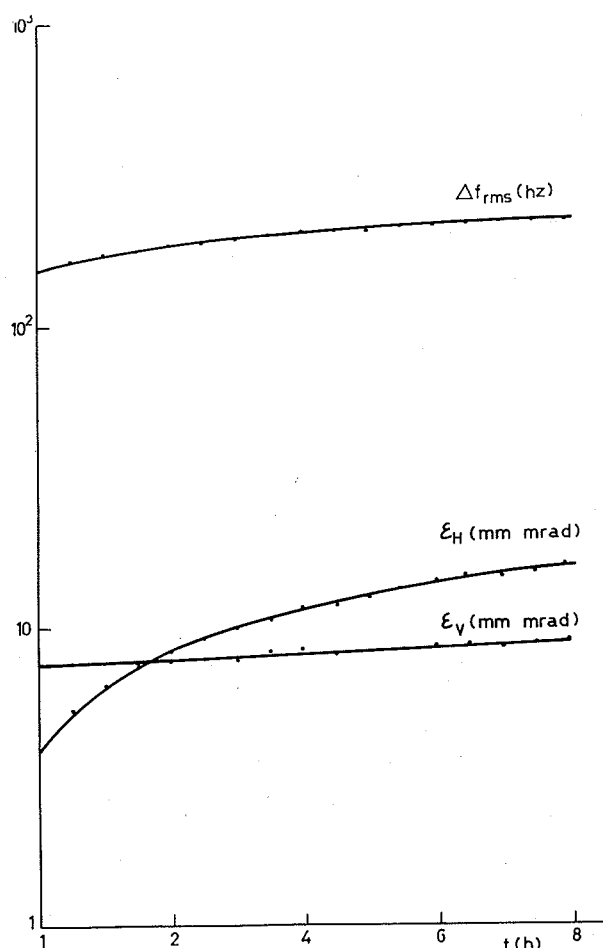

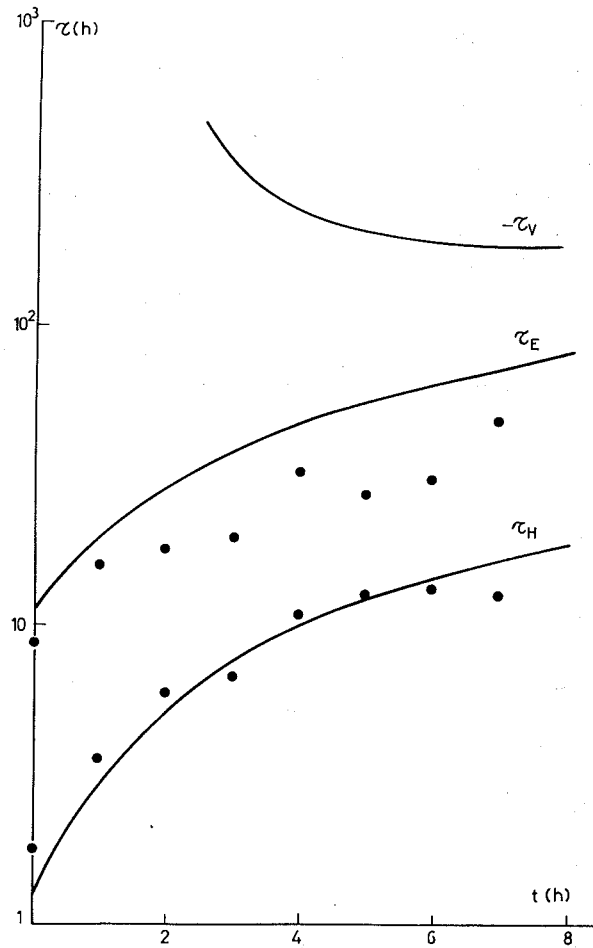FIGURE 5   Plots of the rms stack-with frequency $\Delta f_{rms} = 1.58 \times 10^5 \ (\Delta p/p)_{rms}$ and of the transverse emittances ε_H, ε_V vs time.

FIGURE 6   Plots of measured (dots) and theoretical (solid line) growth rates τ_H, $-\tau_V$, τ_E vs time.

Thereafter, the data are submitted to a linearization procedure for obtaining approximate linear behavior in the vicinity of a given time variable t_i. Thus, the curves of Fig. 5 may be considered piecewise linear over a reasonably short time interval Δt_i of the logarithmic derivatives [see Eqs. (1.a) and (1.b)] of the emittances and of the relative momentum spread with respect to the time. Hence, the desired experimental growth rates $1/\tau_{ai}$ on every portion Δt_i are just the slope of the locally smoothed curves.

Figure 6 shows the measured rise times compared with their corresponding values as predicted by the theory. The observed growth rates are in good agreement with the values obtained by using the generalized intrabeam-scattering model, except for the vertical plane, where the experimental data are somewhat different from the predicted ones.

CONCLUSIONS

Measured data agree rather well with values obtained by using the two different theoretical approaches, provided they are modified as discussed above. The agreement is particularly good for horizontal and longitudinal motions, where rise times have values less than 40 hours.

The discrepancy between theoretical and experimental vertical growth rates is not significant. The fact that absolute values of τ_V are so large implies that they describe a very weak scattering effect. The rate of scattering predicted is therefore rather small and it is not surprising that other phenomena, such as residual gas-multiple scattering, can interfere.

As a final comment, it is worthwhile to emphasize that now the theory of intrabeam scattering has been carefully checked against reliable experimental data, and it can be applied with considerable confidence even to the new low-energy storage-ring projects.

REFERENCES

1. Design Study of an Antiproton Collector for the Antiproton Accumulator (ACOL), edited by E. J. N. Wilson, CERN 83–10.
2. Design Study of a Proton-Antiproton Colliding Beam Facility, CERN/PS/AA 78–3.
3. A. Piwinski, Proc. 9th Int. Conf. on High Energy Accelerators, 1974, p. 405.
4. M. Martini, Intrabeam Scattering in the ACOL-AA Machines, CERN/PS/84–9 (AA).
5. J. D. Bjorken and S. K. Mtingwa, *Particle Accelerators*, **13**, 115 (1983).
6. H. Koziol, Antiproton Accumulator (AA) parameter List, PS/AA/Note 80–1.
7. M. Martini and S. van der Meer, High Intensity Intrabeam Scattering with a Proton Stack, CERN PS/AA/ME/Note 75, 1984.

APPENDIX

The matrices appearing in Eq. (2) are

$$M = L + \lambda I, \quad \text{with} \quad I = \text{unit matrix}, \quad \lambda = \text{eigenvalue of the matrix } L,$$

being

$$L = L^{(H)} + L^{(V)} + L^{(E)},$$

where $L^{(H, V, E)}$ are respectively Eq. (2.37b, d, c) of Ref. 5. In addition

$$A = \frac{NB}{\beta^3 \gamma^4 \sigma_\delta \varepsilon_H \varepsilon_V}, \quad \text{with} \quad B = \begin{cases} \dfrac{5cr_p^2}{\sqrt{\pi}C} & \text{(unbunched beam)} \\[2mm] \dfrac{2.5cr_p^2}{\pi\sigma_s} & \text{(bunched beam)} \end{cases}$$

$\gamma = \text{Lorentz factor} = (1 - \beta^2)^{-1/2}, \ \beta = \text{relativistic velocity}$
$\beta_H = \text{horizontal betatron function}$
$\beta_V = \text{vertical betatron function}$

δ = dispersion or momentum compaction function
σ_δ = standard deviation of the relative momentum spread
σ_s = standard deviation of the bunch length
N = number of circulating particles (either p or $\bar{p}$)
C = ring circumference
c = velocity of light
$r_p = 1.535 \times 10^{-18}$ m = classical proton radius

Tedious and long manipulation of Eq. (2) leads to

$$\frac{1}{\tau_H} = A\left\langle \gamma^2\left(\frac{\delta^2}{\beta_H \varepsilon_H} + \frac{\beta_H}{\varepsilon_H}\phi^2\right)\right.$$

$$\left. \times \int_0^\infty \frac{\left[\left(2a - \frac{\beta_H}{\varepsilon_H} - \frac{\beta_V}{\varepsilon_V} + a_2\right)\lambda + b_1 - 3\frac{\beta_H}{\varepsilon_H}\frac{\beta_V}{\varepsilon_V} + b_2\right]\sqrt{\lambda}\,d\lambda}{(\lambda^3 + a_1\lambda^2 + b_1\lambda + c_1)^{3/2}}\right\rangle \quad \text{(A1)}$$

$$\frac{1}{\tau_E} = A\left\langle \frac{m\gamma^2}{\sigma_\delta^2}\int_0^\infty \frac{\left[\left(2a - \frac{\beta_H}{\varepsilon_H} - \frac{\beta_V}{\varepsilon_V}\right)\lambda + b - 2\frac{\beta_H}{\varepsilon_H}\frac{\beta_V}{\varepsilon_V}\right]\sqrt{\lambda}\,d\lambda}{(\lambda^3 + a_1\lambda^2 + b_1\lambda + c_1)^{3/2}}\right\rangle \quad \text{(A2)}$$

$$\frac{1}{\tau_V} = A\left\langle \frac{\beta_V}{\varepsilon_V}\int_0^\infty \frac{\left[-\left(a + \frac{\beta_H}{\varepsilon_H} - 2\frac{\beta_V}{\varepsilon_V}\right)\lambda + b_1 - 3\frac{\varepsilon_V}{\beta_V}c_1\right]\sqrt{\lambda}\,d\lambda}{(\lambda^3 + a_1\lambda^2 + b_1\lambda + c_1)^{3/2}}\right\rangle, \quad \text{(A3)}$$

where ϕ, a, b and c_1 are respectively Eq. (2.37e) and Eq. (4.8a, b, c) of Ref. 5 and

$$a_1 = a + \frac{\beta_H}{\varepsilon_H} + \frac{\beta_V}{\varepsilon_V}, \qquad b_1 = b + \frac{\beta_H}{\varepsilon_H}\frac{\beta_V}{\varepsilon_V}$$

$$a_2 = \frac{\beta_H}{\varepsilon_H}\left(6\frac{\beta_H}{\varepsilon_H}\gamma^2\phi^2 - a + 2\frac{\beta_H}{\varepsilon_H} - \frac{\beta_V}{\varepsilon_V}\right)\frac{1}{D}$$

$$b_2 = \frac{\beta_H}{\varepsilon_H}\left(6\frac{\beta_H}{\varepsilon_H}\frac{\beta_V}{\varepsilon_V}\gamma^2\phi^2 + b_1 - 3\frac{\beta_V}{\varepsilon_V}a\right)\frac{1}{D},$$

with

$$D = \gamma^2\left(\frac{\delta^2}{\beta_H\varepsilon_H} + \frac{\beta_H}{\varepsilon_H}\phi^2\right).$$

When β_H/ε_H and β_V/ε_V can be neglected with respect to

$$\frac{\gamma^2\delta^2}{\varepsilon_H\beta_H}, \qquad \frac{\beta_H}{\varepsilon_H}\gamma^2\delta^2, \qquad \frac{m\gamma^2}{\sigma_\delta^2},$$

one has $a_1 \simeq a$, $b_1 \simeq b$ and can neglect a_2, $b_2\beta_H/\varepsilon_H$, β_V/ε_V with respect to a and b.

Note that the approximations used in Ref. 5 are valid only for a ring with $\gamma \gtrsim 10$, considerably larger than the stack center value[6] ($\gamma = 3.7722$) of the CERN Antiproton Accumulator.